Original Research Article

QUANTITATIVE INTERPRETATION OF PETROPHYSICAL PARAMETERS FOR RESERVOIR CHARACTERIZATION IN AN ONSHORE FIELD OF NIGER DELTA BASIN

ABSTRACT

Reservoir characterization of a field was performed using petrophysical parameters for the evaluation of subsurface geological features and hydrocarbon potential of an onshore field in Niger Delta Basin. Four reservoir intervals were identified within the field wells based on their position within the stratigraphic column, and the reservoir correlation, which was aided using the principle of uniform horizontality, based on the simple rule that sediments are deposited horizontally and basic understanding of sequence stratigraphy. The study revealed that, the four reservoirs were predominantly sand units intercalated with shale within the reservoir units. The petrophysical evaluation revealed the Net to Gross (NTG) values ranges from 79% to 87% within the reservoir units, while the effective porosity ranges from 17% to 21%, the permeability ranges between 1307mD to 1678mD across the reservoir units, while the water saturation ranges from the lowest of 35% (Reservoir C) to 78% in reservoir D. The approach validates the lithology discrimination of the elastic properties from the well logs and its effectiveness in optimizing and proper understanding of the subsurface, thus identifying and unmasking hidden features within the reservoir (probable bypass) in the field. The study has revealed that petrophysical parameters can be used quantitatively to characterize a field in terms of its lithology and fluid contents of the reservoir.

KEYWORDS: Reservoir Characterization, Cross plots, Discontinuity, Quantitative, Discrimination, Stratigraphic Column.

INTRODUCTION

Since the inception of the oil and gas industry, the need to properly explore for the natural resources using various methods has been a major priority by man, but the recent decline in the prices of oil and gas has increased exploration cost and even halted exploration activities in many oil and gas producing countries, thereby creating financial challenges to most producing and servicing companies, but the ever-increasing demands for fossil fuel energy has triggered a

widespread global research for technologies, which tends to reduce the cost of exploration and improved production rate. The desire to explore more reservoirs and deeper reserves (offshore reservoirs) has implored most oil and gas companies to embraces advance technology in their quest for more hydrocarbon. Thus, most companies will encourage the use of important tools needed for a very careful and thorough evaluation of information obtained from the subsurface. Seismic attributes allow the geoscientists to interpret faults and channels, recognize depositional environments and unravel structural deformation history. They are also useful in checking the quality of seismic data for artifacts delineation, seismic facies mapping, prospect identification, risk analysis and reservoir characterization. Seismic attributes provide a link between petrophysical properties and seismic data of the reservoir, which are directly or indirectly related to rock properties of the field.

In areas where well-log data is unavailable, real and effective estimate of facies distribution and prediction of hydrocarbon reservoir properties can be made based on seismic patterns recognition and correlation (Barnes, 2001; Chen and Sidney, 1997).

This research work was borne out of the fact that there is a need to reduce exploration risk and uncertainties to their barest minimum in the industry, considering the financial cost effects on exploration activities.

Geological Setting of Niger Delta

Structural Overview of Niger Delta Basin

Niger Delta is a large, arcuate delta of the typical, wave- and tidal-dominated type (Doust and Omatsola, 1990). It is located in the Gulf of Guinea on the margin of West Africa, at the southern culmination of the Benue trough and extends from about latitudes 4^0 to 6^0 N and

longitudes 3^0 to 9^0 E (Opara *et al.*, 2011). The delta formed at the site of a rift triple junction related to the opening of the southern Atlantic starting in the Late Jurassic and continuing into the Cretaceous as shown in Figure 1 (*Tuttle et al.,* 1999). During the tertiary, it built out into the Atlantic Ocean at the mouth of the Niger-Benue river system, an area of catchment that encompasses more than a million square kilometers of predominantly savannah-covered lowlands (Weber and Daukoru, 1975). It ranks amongst the world's most prolific petroleum producing tertiary deltas that together account for about 5% of the world's oil and gas reserves (*Opara et. al.,* 2011). The evolution of the Niger Delta is predominantly controlled by pre- and syn-sedimentary tectonics (*Evamy et. al.,* 1978), the formations reflect a gross coarsening-upward progradational clastic wedge (Short and Stauble, 1967), which were deposited either in marine, deltaic, and fluvial environments (Weber, 1986), as accumulation of marine sediments in the basin probably commenced in Albian time, after the opening of the South Atlantic Ocean between the African and South American continents (Doust and Omatsola, 1990). The deposition of the three formations occurred in each of the five offlapping siliciclastic sedimentation cycles that comprise the Niger Delta**, t**hese cycles (depobelts) are 30-60 kilometers wide, prograde southwestward, 250 kilometers over oceanic crust into the Gulf of Guinea (Stacher, 1995).

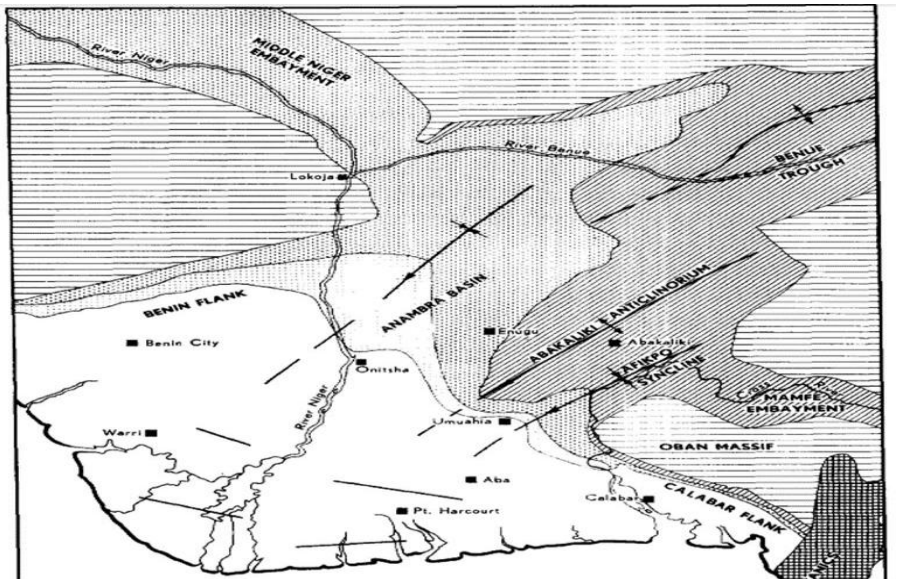

Figure 1: Structural units of Niger Delta Area (Short and Stauble, 1967)

Chronostratigraphy

The Niger Delta basin consists of Cretaceous to Holocene marine clastic strata that overlie oceanic and fragments of continental crust (Figure 2) (Corredor et al. 2005). They also stated that the Cretaceous section has not been penetrated beneath the Niger Delta basin, and thus, Cretaceous lithologies can only be extrapolated from the exposed sections in the next basin to the northeast around the Anambra basin. In this basin, Cretaceous marine clastic consist mainly of Albian–Maastrichtian shallow-marine clastic deposits (Nwachukwu, 1972), while on the other hand, the Tertiary Niger Delta represents a succession of alternating deep-water, shallow marine, and deltaic sands and shales that began prograding onto a passive continental margin as early as Eocene time (*Corredor et al.*, 2005). Sediments has been transported to the delta through the Benue Trough/Bida Basin failed rift system where the total Tertiary section may reach up to 12 km in thickness near the center of the basin (Doust and Omatsola, 1990).

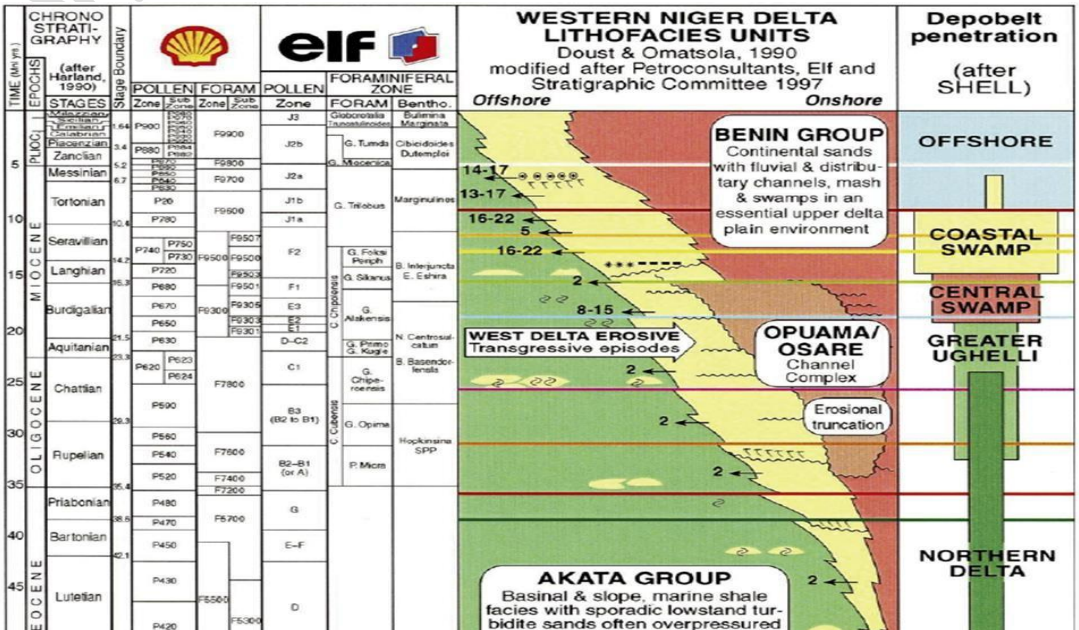

Figure 2: Regional Stratigraphy of Western Niger Delta (Reijers, 2011).

Depobelts

The deposition of the three formations occurred in each of the five offlapping siliciclastic sedimentation cycles that comprise the Niger Delta**, t**hese cycles (depobelts) are 30-60 kilometers wide, prograde southwestward, 250 kilometers over oceanic crust into the Gulf of Guinea (Stacher, 1995). They are well defined by syn-sedimentary faulting that occurred in response to variable rates of subsidence and sediment supply with each depobelt as a separate unit that corresponds to a break in the regional dip of the delta and is bounded landward by growth faults and towards the sea by large counter-regional faults or the growth fault of the next seaward belt (Doust and Omatsola, 1990). Five major depobelts are generally recognized which include the Northern, Greater Ughelli, Central Swamp, Coastal Swamp and Offshore depobelts (Figure 3), each with its own sedimentation, deformation, and petroleum history (*Steele et al,* 2009).

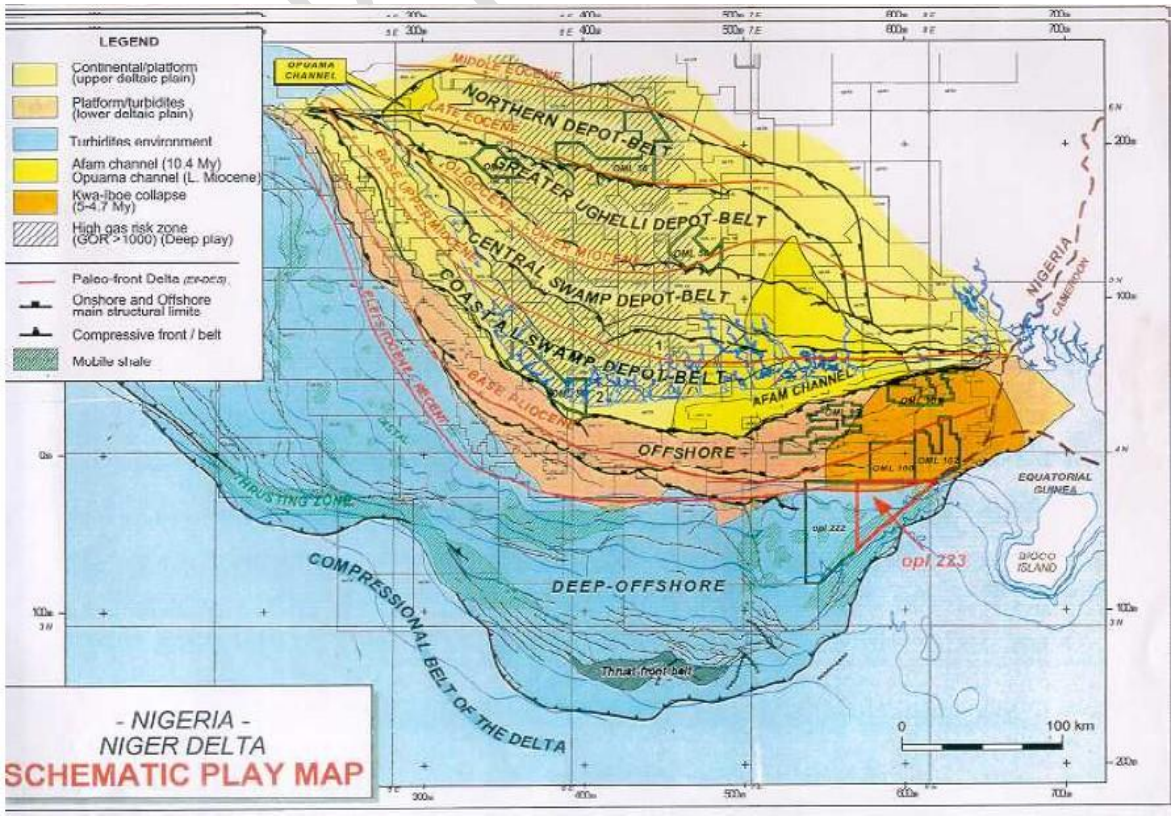

Figure 3: Map Showing the Niger Delta Depobelts (Steele et al., 2009)

LOCATION OF STUDY AREA

The study area is located at A-Field, within the onshore area of Niger Delta in Nigeria (Figure 3). The terrain is generally swampy in nature, with river channels and tributaries emptying into the Atlantic Ocean. The Field lies between longitude 6°17"55'E and latitude 4°37"27'N. The Field is located within the Central Swamp Depobelt, Onshore Niger Delta.

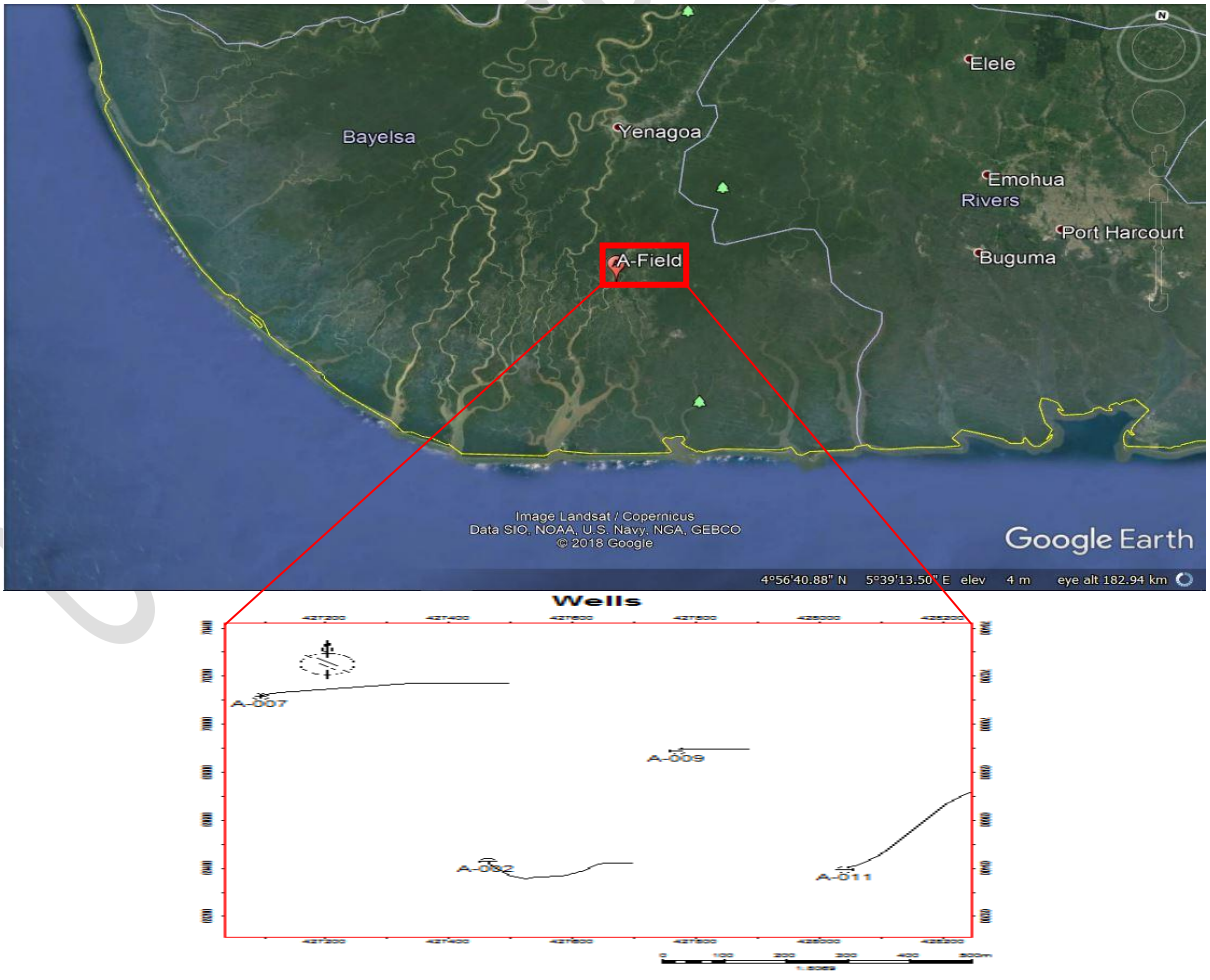

Figure 4: A map showing the location of the A-Field, Central Swamp Depobelt, Onshore Niger Delta (Source: Google Earth 2018) and the Base map for A-Field showing the distribution of wells within the area.

THEORETICAL BACKGROUND:

Well Logs

A well log is a record of measurements of the subsurface formation properties in a well. Well logs data are routinely used for stratigraphic interpretation of the earth's subsurface; it is a practice of making a detailed record of the geologic formations penetrated by a borehole. The logs are based physical measurements made by instruments lowered into the hole, logging of a well can be done during completion, producing or abandoning which is performed in boreholes drilled for oil and gas, groundwater, mineral, and geothermal exploration, as well as part of environmental and geotechnical studies. Well logs are generally prepared in order to evaluate hydrocarbon deposits and some of these logs include gamma ray, sonic, resistivity (deep, medium & shallow), neutron-porosity, density and caliper et cetera.

Types of Well Logs

Gamma Ray Logs

This is the measurement of the natural radioactivity in a formation or response to the presence of uranium, potassium- and thorium-rich minerals in the formation. As the clay content increases, the gamma ray response increases; organic-rich marine shale commonly has the greatest

response as it contains significant amounts of uranium-rich minerals generated by the reduction of decaying organic matter. The GR is used primarily to define the volume of shale (*V*sh) in a sequence, especially where the self-potential (SP) response is distorted or where oil-based mud is being used. When comparing GR logs from a number of wells, they should all be normalized to a common scale, as each tool will have been calibrated individually. This is especially true if being used for correlation or quantitative calculations.

Porosity Logs

This measures the ratio of the volume of pore (void) space (*V*p) to the total volume of rock (*V*t), which can be described as primary or secondary porosities depending on whether mineral dissolution has occurred during lithification. Porosity can also be classified as either total (PhiT) or effective (PhiE), depending on the source of the measurement; core data are generally assumed to be 'total' because of the cleaning and drying process in the laboratory, but a log-derived measurement could be either effective or total depending on how it has been derived. A number of logs measure porosity, although none actually does this directly, three common tools exist namely the sonic log, which measures the acoustic response of a formation while the density and neutron logs takes nuclear measurements. When these tool responses are combined, two or three at a time, lithology can also be determined, along with a representative porosity interpretation.

- **Sonic Log**

The sonic log measures the interval transit time of a compressional sound wave traveling through the formation along the axis of the borehole wall, a compressional sound wave can travel in solids, liquids and gases; however, the fastest path for the wave to follow is through the solid. The interval transit time (Δt) is the reciprocal of the velocity of the sound wave passing through

the formation and is measured in microseconds per foot or metre (μs/m or μs/m). Sonic logs can be mathematically derived from:

$$\emptyset_{Sonic} = \frac{\Delta t \log - \Delta tma}{\Delta t_f - \Delta tma} \times \frac{1}{C_p} \quad (1)$$

ϕ_{Sonic} = Sonic derived porosity

Δt_{ma} = interval transit time of matrix (given)

Δt_{log} = Interval transit time of formation

Δt_F = Interval transit time of fluid in the well bore (Fresh mud = 189, salty mud = 185)

$$C_p = \frac{\Delta t_{sh} \times c}{100} \quad (2)$$

C_p = compaction factor

Δt_{sh} = Interval transit time of adjacent shale

C = a constant, normally 1.0 (Hilchie, 1978)

- **Density logs**

The density log measures the bulk density of the formation; that is, the density of the rock plus the fluids contained in the pores. Density is measured in g/cm^3 and is by convention given the symbol ρ (rho). Porosity value can be estimated using the density tool, it is necessary to know the matrix density and the density of any fluids in the pore space. Porosity from the density log is calculated using the equation.

$$\emptyset_{Den} = \frac{\rho ma - \rho_h}{\rho ma - \rho_f} \quad (3)$$

ϕ_{Den} = Apparent density porosity

ρ_{ma} = Matrix density

ρ_b = Bulk density log reading

ρ_f = Fluid density (1.1 salt mud, 1.0 fresh mud and 0.7 gas)

- **Neuron Log**

Neutron logs measure the hydrogen concentration in a formation, the hydrogen index (HI) from its commonest source of hydrogen in the formation which are water or hydrocarbons. In shale-free rocks where the pore space is filled with water or oil, the neutron log directly measures liquid-filled porosity and where the pores are filled with gas the concentration of hydrogen is reduced, resulting in a lower porosity reading from the tool, which is called the gas effect. The neutron porosity is calculated directly from the log response, as the tool measures liquid-filled porosity; it is usually calibrated in limestone porosity units and must, therefore, be corrected for the actual lithology. The relationship between the neutron count rate and porosity can be expressed mathematically as

$$\log_{10} \emptyset = aN + B \quad (4)$$

a = constant

B = constant

N = count rate and ϕ is the true porosity.

Resistivity Logs

This is used to measure the subsurface electrical resistivity which helps to differentiate between formations filled with salty waters (good conductors of electricity) and those filled with hydrocarbons (poor conductors of electricity). Resistivity log measurement is very important in the determination of hydrocarbon and when combined with porosity logs, they can be used to calculate hydrocarbon saturation and to delineate potential reservoirs. The resistivity of the formation depends on the pore geometry, fluid present in the formations with a high possibility

of obtaining hydrocarbon but lower readings show the presence of water due to its conductivity, it is expressed in ohms. Resistivity logs includes Micro-logs normal/inverse, Micro-Laterolog, Proximity log, Micro-Spherically Focused log, Laterolog, and Induction log.

Petrophysical Properties

Petrophysics is a study of the physical and chemical properties of rock and their interactions with fluids. It is majorly applied in the study of reservoirs for the hydrocarbon industry and some of the key properties studied are Gross and Net thickness, porosity, fluid saturation, permeability, Net to Gross ration and shale volume. A key aspect of petrophysics is measuring and evaluating these rock properties by acquiring well log measurements. The petrophysical properties are as follows:

Gross and Net thickness

The gross thickness of the reservoir is the entire thickness of the reservoir, including the shaly sections of the reservoir while the net sand is the interval of sand in the reservoir that is clean, containing no shaly fractions. The net sand can be computed after the Volume of shale has been determined and subtracted from the total reservoir thickness.

Porosity

Porosity may be defined as *effective* or *total* depending on whether it includes porosity associated with clays; some tools measure total porosity and must be corrected for the clay content.

Total porosity (Φ_T) and effective porosity (Φ_E) were calculated based on Wyllie's equation as follows;

$$\emptyset_T = \frac{\rho_{ma} - \rho_{bulk}}{\rho_{ma} - \rho_{fl}} \quad (5)$$

$$\emptyset_E = \emptyset_T - (\emptyset t_{sh} \times Vsh) \quad (6)$$

Where;

Φ_T = density derived porosity

ρ_{ma} = matrix density taken as 2.65g/cm^3

ρ_{bulk} = matrix density taken as bulk density log values

ρ_{fl} = fluid density taken as 1.00g/cm^3

V_{sh} = Shale volume

Φ_{tsh} = Total porosity of shale

Fluid Saturation

Fluid saturation in petrophysics comprises of both water and hydrocarbon saturation contents. Water saturation (*S*w) is the proportion of total pore volume occupied by formation water; for water saturation (Sw), from Archie's (1942) empirical equation was utilized as follows;

$$\text{Sw} = \left(\frac{a \times R_w}{R_t \times \emptyset_t^m}\right)^{1/n} \quad (7)$$

Where;

S_{wa} = Archie's water saturation for clean sand
a = Tortuosity factor that is 1
m = Cementation exponent which is 2
n = Saturation exponent that is 2
Rt = Formation resistivity (read from log)
Rw = Formation water resistivity (read from log)
Φ_t = Total Porosity

Hydrocarbon saturation is the proportion of fluid that is (oil and gas) and is derived from the relationship

$$S_H = 1 - S_w. \quad (2.8)$$

Permeability

Permeability (*k*) is the measurement of the capacity of a reservoir to conduct fluids or its ability to allow flow to take place between the reservoir and a wellbore; which also dependent on the associated rocks and fluid properties. Permeability occur as effective permeability (K_{eff}), which is the permeability of one liquid phase to flow in the presence of another; relative permeability (*K*r), the ratio of effective to absolute permeability for a given saturation of the flowing liquid (i.e. permeability of oil in the presence of water (K_{ro})) and absolute permeability. Permeability is measured in Darcies (D) and can be calculated using the equation given as (Owolabi *et al., 1994)*:

$$K(mD) = 307 + 26552\,(\emptyset^2) - (\emptyset \times S_w)^2 \quad (2.9)$$

Net-To-Gross (NTG)

This is the total amount of pay footage divided by the total thickness of the reservoir. It can be calculated as the oil initially in place (OIIP) or Gas initially in place (GIIP), assuming that the entire reservoir interval is used to determine the total volume of hydrocarbons present within the reservoir interval. Net-To-Gross is a measure of the potential of the productive part of a reservoir. It is usually expressed either as a percentage or fraction of the producible (net) reservoir within the overall (gross) reservoir packages. The higher the Net to Gross, the better the reservoir quality and it is expressed as:

$$\text{Net-to-gross} = \frac{NT}{GT} \times 100 \quad (2.10)$$

NT = Net thickness

GT = Gross Thickness

Shale Volume

This is the space occupied by shale or the fraction of shale (clay) present in reservoir rocks, the volume of shale in a reservoir plays a key role in hydrocarbon production where the higher the reservoir shaliness, the poorer the reservoir productivity. The magnitude of the gamma ray count in a formation of interest is related to the shale content of the formation and the relationship may be linear or non-linear. Shale volume is often calculated using Larionov's equation (1969) for tertiary sands as follows;

$$Vsh = 0.083 * (2^{(3.7 * GR_{index})} - 1 \qquad (2.11)$$

Where

$GR\log = GR\log reading$

$GR\min = GR\ sand\ baseline$

$GR\max = GR\ shale\ baseline$

METHODOLOGY

MATERIALS AND METHODS

This study was conducted using well log data obtained (recorded) from an onshore field, in Niger Delta Area (study area). Some of the available data are the well log suite, which comprises of Gamma ray (GR) logs, Caliper logs, Porosity logs (neutron, density and sonic) and resistivity (shallow and deep) with their well header information, check shot data and well survey deviation data. Two major industrial softwares were used for the processing and interpretation.

Research Design and Workflow

The following outlined workflow was utilized for the study as shown in Figure 5:

1. Data sourcing, data gathering, and data loading into relevant software.
2. Data quality assurance and quality control.
3. Well logs conditioning (despiking and interpolation).
4. Well correlation.
5. Petrophysical evaluation of reservoirs.
6. Attribute cross plots from well logs
7. Hydrocarbon Prospect evaluation
8. Volumetric evaluation.

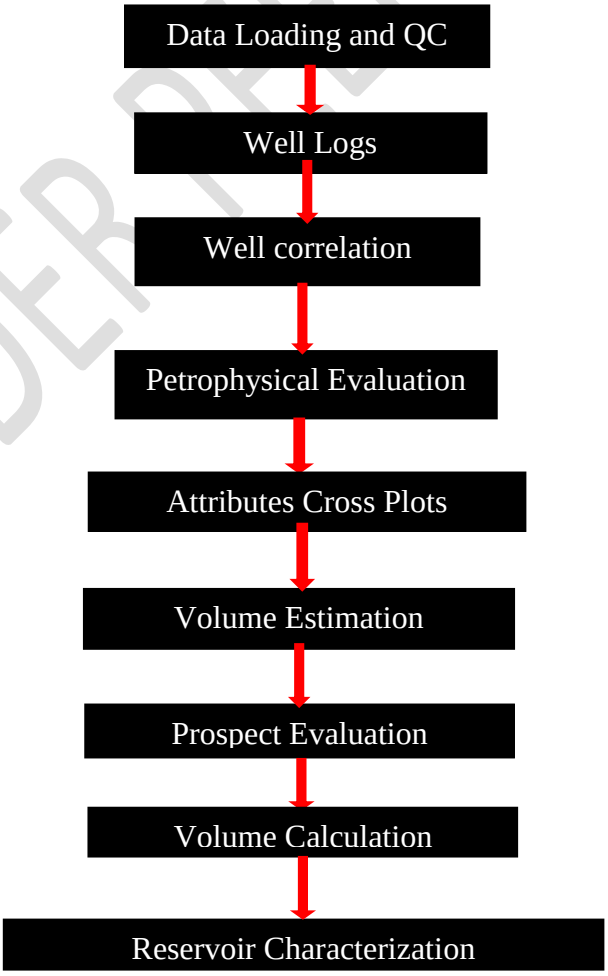

Figure 5: Workflow utilized for the analysis of A-Field

Methods:

The data set were quality checked and sorted into acceptable format for the software namely: Petrel^{TM} software which was used for data appraisal, well correlation, petrophysical analysis and evaluation, as well as generation of hydrocarbon prospect while the Hampson Russell software was used for lithology evaluation and fluid discrimination respectively.

Prior to loading the data into the respective softwares, the project geographic reference zone, coordinates, and units were determined and set. The well header information was uploaded; this contains the names of all the wells, their geographic references, the total drilled depth and also the well reference datum. A total of 4 wells were available and utilized for this study which included; Well A-002, A-007, A-009, and A-011 as shown on the base map (Figure 4), the wells distributions were not even across the area. The well deviation, which defines the trajectory of the well, shows the heterogeneity of geologic layers.

Well logs were available, Gamma Ray log in gAPI unit, Deep Resistivity in Ohm.m, Density in g/cm^3, Neutron in m^3/m^3 and Sonic in µs/m. All well log depths were available in feet.

Table 1: Well data inventory for four wells utilized in this study.

Well Name	Well logs						Well Header	Check shot	Directional Survey
	GR	Cali	Res	Den	Neutron	Sonic			
A-002	YES	YES	YES	YES	YES	YES	YES	NO	YES

A-007	YES	YES	YES	YES	YES	YES	YES	NO	YES
A-009	YES	YES	YES	YES	YES	YES	YES	NO	YES
A-011	YES	YES	YES	YES	YES	YES	YES	YES	YES

The Gamma ray log differentiated the lithology into sand and shale, high resistivity log readings identified sand zones for hydrocarbon accumulation and low resistivity readings indicated shale zone. A cross plots of neutron and density logs were performed to characterize the fluid content in the reservoir in order to indicate areas of hydrocarbon

Checkshot data provided was for well A-011 only, which was loaded and displayed in a function window for conditioning by displaying as a graph with depth on the vertical axis and TWT on the horizontal axis to check for any spikes not related to geology. There was no spike (outlier), hence the checkshot was of good quality.

Well Logs Correlation

Correlation was done between the wells to identify specific reservoir formations encountered within the different wells; the well correlation identification was achieved with the aid of gamma ray log measurements. The GR scale was set from 0 to 150 gAPI on the GR tract, based on the defined cut-off, GR deflections to the right of the cut-off defined clean sand whereas deflections to the left of the tract defined shales. Three stacking patterns identified for correlation and identification of depositional environment in the field includes; progradational (bell-shaped), retrogradational (funnel-shaped) and aggradational (blocky).

Fluid Contact Delineation

The oil water contact (OWC) was determined with the aid of the resistivity log based on the fact that oil is more resistive than brine; there was a sharp rise in resistivity, which indicates the presence of hydrocarbons in the reservoir in the resistivity logs. Meanwhile, neutron and density logs were used to ascertain the type of hydrocarbon presence in the reservoirs. Oil zones were majorly identified due to the effect of the cross over between neutron and density logs which showed a small separation.

Petrophysical Properties Estimation

The petrophysical parameters for the reservoir zones in the different wells were calculated using the relevant equations given above. The following petrophysical parameters were estimated namely; fluid saturation (water and hydrocarbon saturation), shale volume, permeability, porosity (total and effective), these values were plotted in the log sections.

Extracted Attributes Cross Plots Analysis

In order to delineate the extent and determine the volume of hydrocarbon in-place in probable reservoirs identified in the wells, some of the attributes from well logs were estimated and cross plotted (using 3-D cross plots), where the 3rd dimension connotes the colour coding of the data points using Hampson-Russell software. Three major attributes of the well data were estimated and used to delineate the lithology and the discrimination fluid contents in the reservoir , which includes two lame's paraments (elastic moduli), namely Lambda-rho (incompressibility modulus - $\lambda\rho$) and Mui-rho (rigidity modulus - $\mu\rho$) and the acoustic impedance.

$$\text{Lambda-Rho } (\lambda\rho) = (\text{P-impedance})^2 - C \times (\text{S-impedance})^2 \quad (3.1)$$

$$\text{Mui-Rho } (\mu\rho) = (\text{S-impedance})^2 \quad (3.2)$$

P-impedance = P-wave x Density (3.3)

RESULTS AND DISCUSSION

The results obtained from the study, which includes results from the well log evaluation of the selected wells, delineation of the well lithology, correlation of the wells, petrophysical analysis and evaluation of the properties and cross-plot analysis for computing the attributes for fluid discrimination are presented in the following Figures 6-12. The results of this study are presented in the following order; well log evaluation of the selected wells, well correlation, petrophysical parameter analysis, cross plot for attributes computed to identify lithology and fluid discrimination, and volumetric estimation. These obtained reservoirs parameters were used for petrophysical evaluation of the reservoir properties, namely Shale Volume, Effective porosity, Permeability, Water and Hydrocarbon saturation as shown in the Figures 8-11, while the estimated values are tabulated in Table 1. The fluid contents in the reservoir sand units were discrimination using the resistivity log and the cross plot analysis.

Well Log Evaluation

Based on the gamma ray logs, two lithologies were identified; sand and shale. From the gamma ray log, the interval coloured yellow is identified as sand due to low value in gamma ray, while the gray-yellow for shale is as a result of high gamma ray readings. The gamma log signatures indicate areas with sand and shale. The resistivity log signatures indicate a higher value at a point where the gamma ray logs reading is low (where there is sand) and the high resistivity indicates brine sand. The cross plot of density and neutron log signatures conform to the gamma ray log

readings indicating oil and water zones in the reservoir as the reservoir consist mainly of oil and water with little or no gas present.

Well Correlation

Four lithologic reservoirs were identified from the results of the correlation as the reservoirs of interest for this study, Reservoir A (A-002), B (A-007), C (A-009), and D (A-011) based on gross thickness and presence of significant pay thickness with reservoir tops ranging from 3288.84m to 3698.26m for well A-002, 3279.63m to 3495.56m for well A-007, 3324.77m to 3542.24m for well A-009 and 3318.15m to 3530.90m for well A-011 respectively, while the reservoir base depths were taken at 3357.86m to 3698.26m for well A-002, 3352.23m to 3683.57m for well A-007, 3389.06m to 3660.44m for well A-009, and 3384.34m to 3720.01m for A-011 respectively as shown in Figure 6a-d.

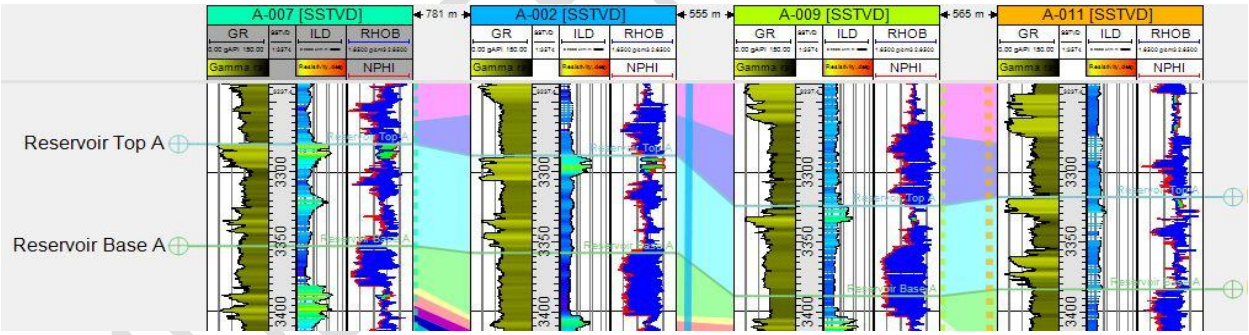

Figure 6a: Identification and correlation of Reservoir A

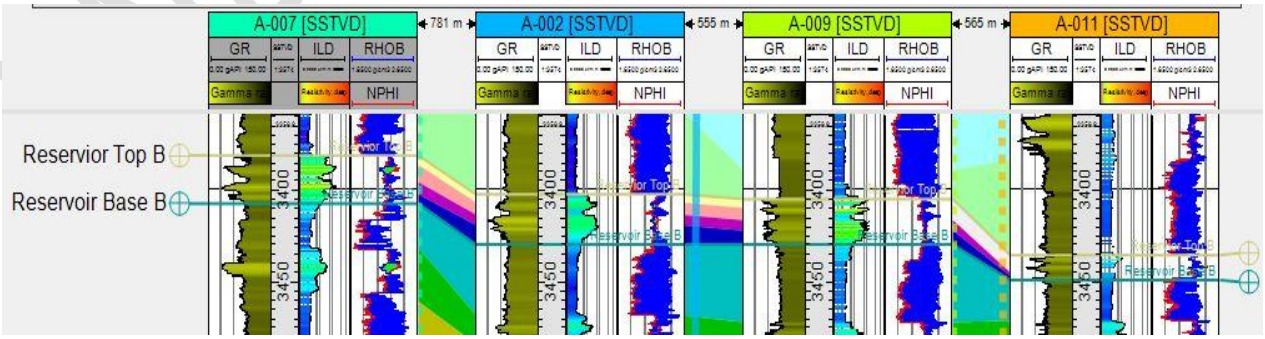

Figure 6b: Identification and correlation of Reservoir B

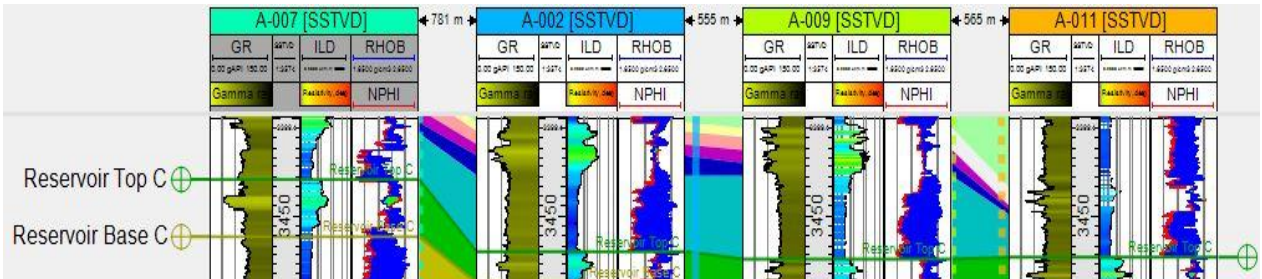

Figure 6c: Identification and correlation of Reservoir C

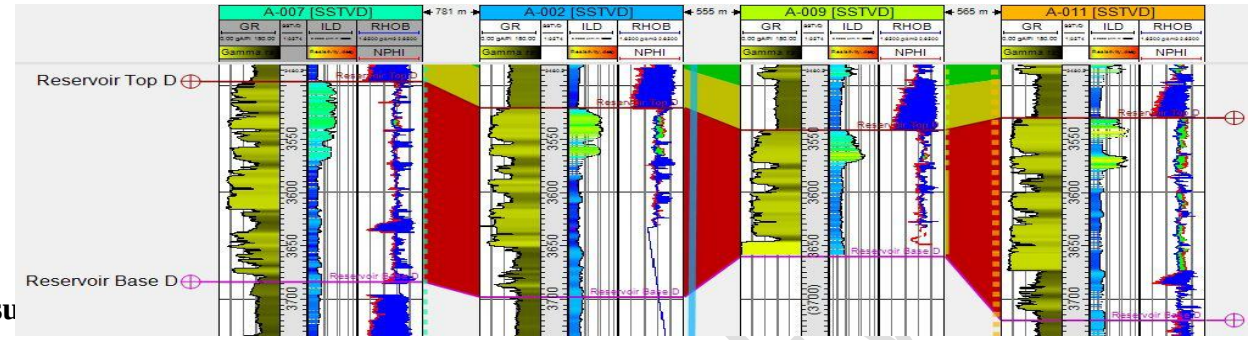

Resu

The results of the petrophysical evaluation estimated for the identified reservoirs in A-field are presented in Table 2, while Figure 7 shows the petrophysical logs derived from the available conventional well logs.

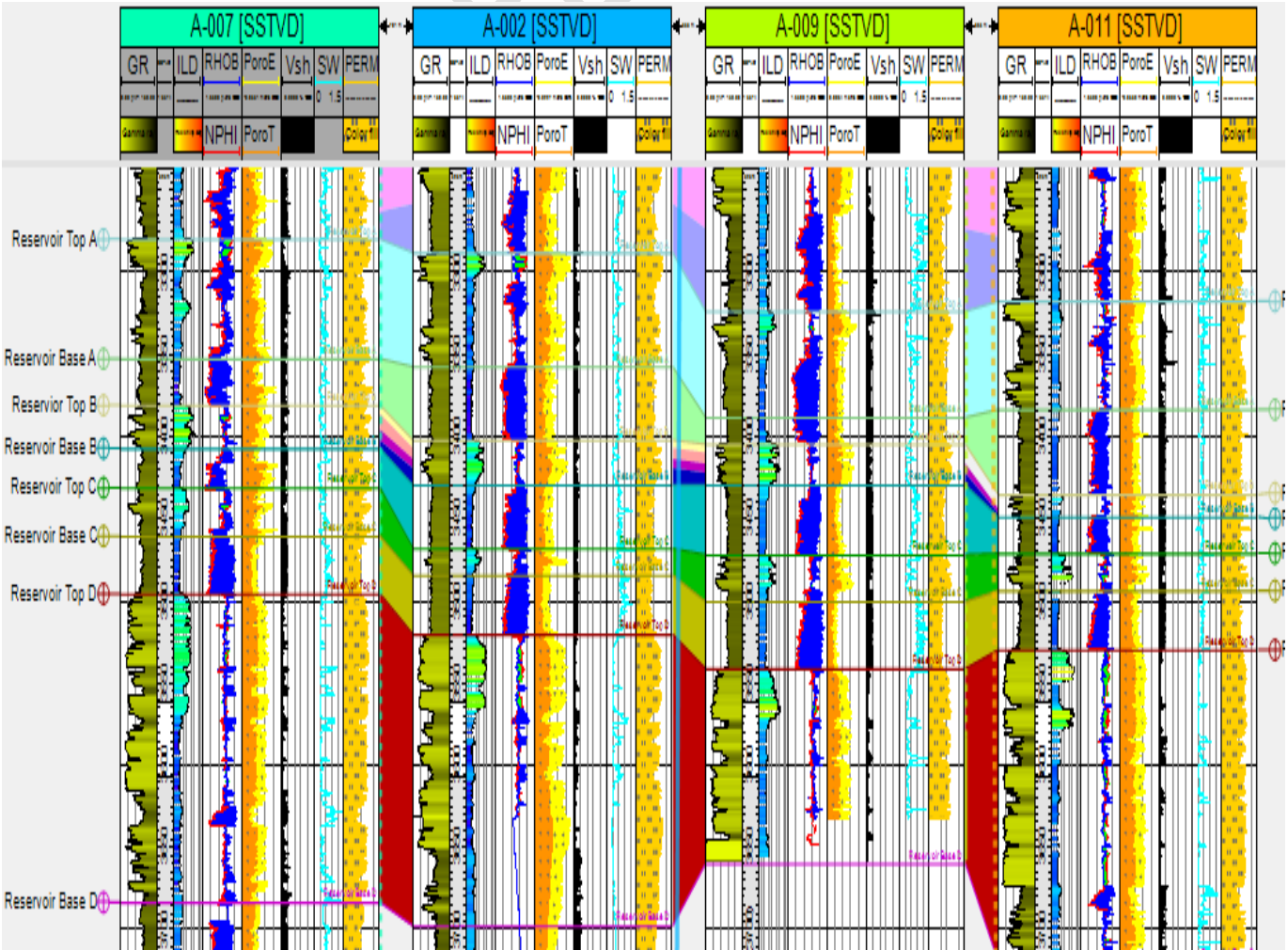

Figure 7: The Correlated wells showing the estimated petrophysical parameters.

Table 2: Results of Petrophysical Evaluation of Three Reservoir Units for Four Wells in the A-field.

Wells	Reservoir sands	Top (m)	Base (m)	Gross thickness (m)	Shale volume (%)	Shale volume (m)	Net sand (m)	Net-to Gross (%)	Total Porosity (%)	Effective Porosity (%)	Water saturation (%)	Permeability (mD)	Hydrocarbon saturation (%)	Fluid type
Well 002	A	3289	3358	69	14%	9.66	59.34	86%	22%	20%	59%	1744.303	41%	Oil/water
	B	3402	3431	29	12%	3.48	25.52	88%	19%	17%	56%	1155.55	44%	Oil/water
	C	3469	3485	16	12%	1.92	14.08	88%	13%	11%	82%	691.9105	18%	Oil/Water
	D	3521	3698	177	13%	23.01	153.99	87%	20%	19%	78%	1636.715	22%	Oil/Water
Well 007	A	3280	3352	72	17%	12.24	59.76	83%	24%	22%	42%	1540.439	58%	**Oil**
	B	3381	3407	26	14%	3.64	22.36	86%	25%	21%	52%	1821.868	48%	**Oil/Water**
	C	3431	3460	29	13%	3.77	25.23	87%	28%	25%	41%	2019.133	59%	**Oil**
	D	3496	3684	188	14%	26.32	161.68	86%	26%	22%	82%	2214.002	18%	**Oil/Water**
Well 009	A	3325	3389	64	23%	14.72	49.28	77%	25%	23%	35%	2037.376	65%	**Oil**
	B	3404	3430	26	13%	3.38	22.62	87%	19%	17%	66%	1254.444	34%	**Oil/Water**
	C	3472	3501	29	14%	4.06	24.94	86%	15%	14%	56%	1001.586	28%	**Oil/Water**
	D	3542	3660	118	13%	15.34	102.66	87%	15%	14%	76%	995.2449	24%	**Oil/Water**

Well 011	A	3318	3384	66	30%	19.8	46.2	70%	19%	16%	78%	1313.773	22%	**Oil/Water**
	B	3435	3449	14	15%	2.1	11.9	85%	19%	16%	51%	991.2469	49%	**Oil/Water**
	C	3471	3494	23	14%	3.22	19.78	86%	29%	24%	44%	2276.725	56%	**Oil**
	D	3531	3720	189	16%	30.24	158.76	84%	19%	17%	81%	1434.346	19%	**Oil/Water**

Gross Thickness

The gross thickness of a reservoir is the entire thickness from the top of the reservoir to the base of the reservoir (Figure 7). The thickness of the reservoirs varies from one well to the other across the field. The thickness of reservoir A is 69m in well A-002, 72m in A-007, 64m in A-009 and 66m in well A-011 (Table 2). Reservoir B has a thickness of 29m in well A-002, 26m in A-007, 26m in A-009 and 14m in well A-011. The thickness of reservoir C is 16m in well A-002, 29m in A-007, 29m in well A-009 and 23m in well A-011 and reservoir D is 177m in well A-002, 188m in A-007, 118m in well A-009 and 189m in well A-011. On average, the gross thicknesses of the reservoirs are: reservoir A is 67.75m, reservoir B is 23.75m, reservoir C24.25m and 168m for reservoir D respectively. The average gross thickness of the reservoirs shows that reservoir D has the highest thickness while reservoir B has the lowest thickness. These results show that the reservoir sands are of sufficient thickness to accumulate hydrocarbons in economic quantities.

Shale Volume (Vsh)

Shale volume is the percentage of shale contained within the reservoir. The higher the shale content the poorer the reservoir quality to yield hydrocarbons. In reservoir A, shale volume ranges from 14-30% across the four wells and accounts for a thickness of 9.66m of the entire

gross thickness in A-002 well, 12.24m in A-007 well, 14.72m in A-007 well and 19.8m in A-011 well (Table 2), while in reservoir B, shale volume ranges from 12-15% in the wells. Quantifying the shale volume in terms of thickness shows that 3.48m, 3.64m, 3.38m, and 2.1m are the thicknesses of shales in reservoir B in the wells respectively (Table 2). The shale volume in reservoir C ranges from 12-14% across the well, which translates to a thickness of 23.01m, 3.77m, 4.06m and 3.22m in A-002, A-007, A-009, and A-011 respectively and for reservoir D, the values ranges from 13-16% across the wells, which translates to a thickness of 23.01m, 26.32m, 15.34m and 30.24m in A-002, A-007, A-009, and A-011. On average, shale volume thickness is 14.11m in reservoir A, 3.15m in reservoir B, 3.24m in reservoir C, and 23.73m in reservoir D (Figure 8). This suggests that about 14.11m of the average gross thickness in reservoir A is occupied by shale, 3.15m of the average gross thickness of reservoir B is occupied by shale, 3.24m of the average gross thickness of reservoir C is shale, while 23.73m of the average gross thickness of reservoir D is shale.

Net Thickness

The reservoir net thickness is the proportion of the reservoir (clean sand) that can be produced. The net reservoir thickness is obtained after the shale volume is removed from the overall gross volume of the reservoir. The net sand thickness of reservoir A is 59.34m in A-002 well, 59.76m in A-007, 1661.68m in A-009 and 46.2m in A-011 well (Table 2). In reservoir B, the net sand thickness is 25.52m in A-002 well, 22.36m in A-007, 22.62m in A-009 and 11.9m in A-011 well respectively. Similarly, reservoir C has a net sand thickness of 14.08m, 22.36m, 24.94m and 19.78m in A-002, A-007, A-007, and A-011 wells then reservoir D has a net sand thickness of 153.99m, 161.68m, 102.66m and 158.76m in A-002, A-007, A-007, and A-011 wells

respectively. The average net sand (clean sand) thickness for reservoir A is 53.65m, 20.6m for reservoir B, 21.01m for reservoir C and 144.27m for reservoir D (Figure 6).

Net-To-Gross

The net to gross is the ratio of the thickness of the clean sand (net sand thickness) divided into the total gross thickness of the reservoir. The net to gross gives an indication of the total amount of the reservoir section that can be produced, the larger the net to gross value (in percentage), the better the quality of the reservoir. For Reservoir A, net to gross ratio ranges from 70-86% across the wells (Table 2), while for reservoir B, the value of net to gross ratio ranges from about 85-88% in the wells. Similarly, for reservoir C, the net to gross ratio ranges from 86-88% across the wells and for reservoir D, the value falls between a net to gross of 84-87% in the wells. The average net to gross ratio for reservoir A, B, C, and D ranges from 79-86.75% respectively (Table 2), this results show that on average, over 84.56% of the entire gross thickness of the reservoirs can be produced if they contain hydrocarbons.

Porosity

Total porosity is the sum total of both the interconnected pores and the isolated pore spaces (Figure 9). The porosity relevant for hydrocarbon production is the effective porosity. The effective porosity is the sum of all the interconnected pore throats. In this study, the result of total porosity for reservoir A is 22% in A-002 well, 24% in A-007, 25% in A-009 and 19% in A-011 well (Table 2), while the effective porosity is 20%, 22%, 23% and 16% in respectively in the wells (A-002, A-007, A-009 and A-011). For reservoir B, total porosity are 19%, 25%, 19% and 19% respectively, while the effective porosity are 17% for A-002, 21% for A-007, 17% for A-009 and 16% for well A-011. Similarly, for reservoir C, total porosity is 13%, 28%, 15% and

29% while effective porosity is 11%, 25%, 14% and 24% for A-002, A-007, A-009 and A-011 wells and for reservoir D, total and effective porosity are 20% and 19% for well A-002, 26% and 22% for A-007, 15% and 14% for A-009 and 19% and 17% for well A-011 respectively. The average total and effective porosity for reservoir A is 22.5% and 20.25%, 18% and 17.75% for reservoir B, 21.25% and 18.5% for reservoir C and 20% and 18%, and for reservoir D respectively (Figure 9). According to Rider classification (1986), porosity measurements <5% are considered negligible, between 5-10% are poor, >10-20% are good, >20-30% are very good and >30 are excellent. Based on this classification scheme which is globally accepted for porosity classification, the total porosity recorded from reservoirs B and D are classed as good, while reservoirs A and C are classified as very good while effective porosity recorded for reservoir A, B, C and D are classed as good.

Permeability

Permeability is the ability of fluids to flow through a reservoir rock. Figure 10 shows the permeability measurements calculated in this study. The results of permeability for reservoir A is 1744.303mD in A-002 well, 1540.439mD in A-007, 2019.133mD in A-009 and 1313.773mD in A-011 well (Table 2). For reservoir B, permeability is 1155.55mD, 1821.868mD, 1254.444mD and 991.2469mD in A-002, A-007, A-009, and A-011 wells respectively. For reservoir C, permeability values are 691.9105mD, 2019.133mD, 1001.586mD and 2276.725mD in A-002, A-007, A-009, and A-011 wells, while for reservoir D, the values are 1636mD, 2214mD, 996mD, and 1434mD respectively. On average, permeability values are 1658.9728mD, 1305.7772mD, 1497.338625mD, and 1570.0770mD in reservoirs A, B, C and D respectively (Figure 10). Rider (1986) classification of reservoir quality based on permeability values are as follows; < 10mD (poor to fair), >10-50 mD (moderate), >50-250 mD (Good), >250-1000 mD (very good) and

>1000 mD (excellent). Based on this classification scheme, reservoir A, reservoir B, reservoir C and reservoir D can be classed as very good to excellent reservoirs because they have average permeability values ranges >1000mD. These results show that all the reservoirs in the field have very good to excellent permeability values which are necessary requirements for hydrocarbon flow and production in economic quantities.

Fluid Type

The three possible fluids that can exist in the pore spaces of reservoirs which accumulated over time due to migration, timing, good sealing mechanism and a trap formed from its source, could be gas, oil and water (fresh or brine) or a combination of two of either. The resistivity log was used to determine the presence of oil and water in the reservoirs due to the fact that oil is more resistive than water. In this study, reservoir A is oil and water bearing in well A-002, A-011 and Oil bearing in A-007, A-009, while reservoir B is oil and water bearing in all the wells (Table 2). Reservoir C, is oil and water bearing in A-002, A-009, while A-007and A-011 are oil bearing only, while in reservoir D, wells A-002, A-007, A-009, and A-011 are all oil and water bearing. These results show that all the reservoir intervals are hydrocarbon bearing and can be produced.

Fluid Saturation

The fluids saturation in the reservoirs was determined using Archie's equation and the logs generated are presented in Figure 11. Water saturation calculated for reservoir A are 59% in A-002 well, 42% in A-007, 35% in A-009 and 78% in A-011 well. This accounts for an equivalent hydrocarbon saturation of 41%, 58%, 65% and 22% respectively (Table 2). For reservoir B, water saturation is 56% in A-002, 52% in A-007, 66% in A-009 and 51% in A-011 well, resulting in an equivalent hydrocarbon saturation of 44%, 48%, 34% and 49% respectively. In

reservoir C, water saturation values are 82%, 41%, 56% and 44% in A-002, A-007, A-009, and A-011 wells respectively. Accordingly, hydrocarbon saturation in reservoir C is as follows; 18%, 59%, 28% and 56% respectively, while in reservoir D, water saturation computed were 78%, 82%, 76% and 81% in A-002, A-007, A-009, and A-011 wells and the corresponding hydrocarbon saturation are 22%, 18%, 24% and 19% in A-002, A-007, A-009, and A-011 wells. The average hydrocarbon saturation values for reservoirs the reservoirs A, B, C and D are 46.5%, 43.75%, 40.25% and 20.75% respectively. These results show that reservoir A has the highest hydrocarbon saturation while reservoir D has the least hydrocarbon saturation measurement (Figure 11) and Table 2.

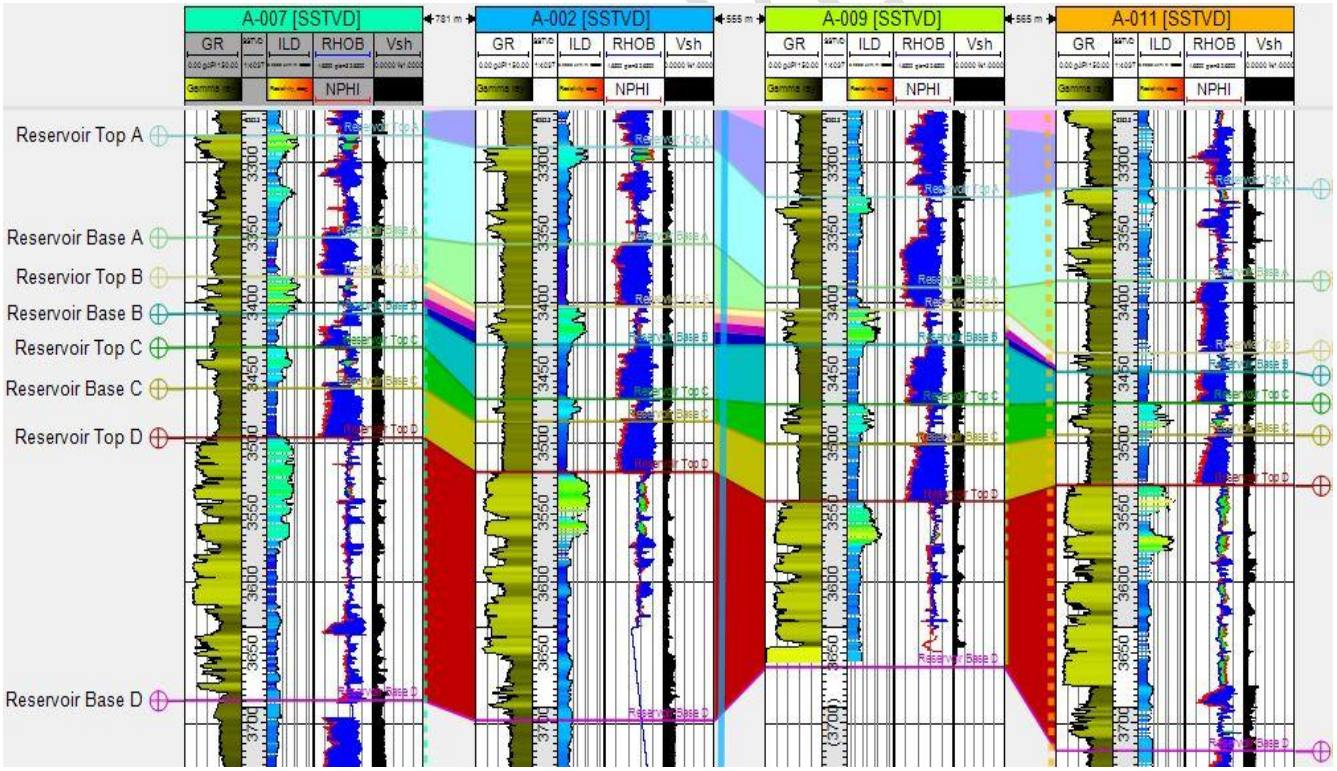

Figure 8: Shale volume values calculated for the four reservoir intervals and correlated across all four wells.

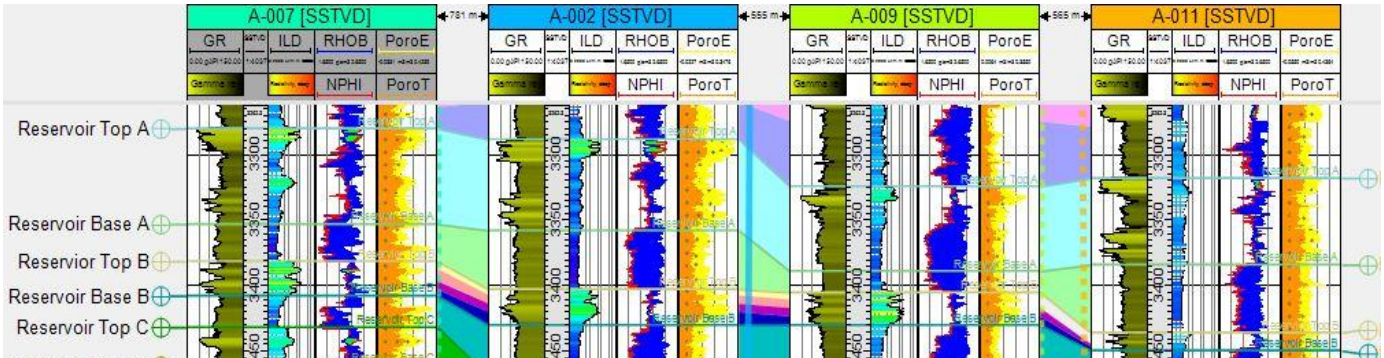

Figure 9: Porosity values calculated for the four reservoir intervals and correlated across all four wells.

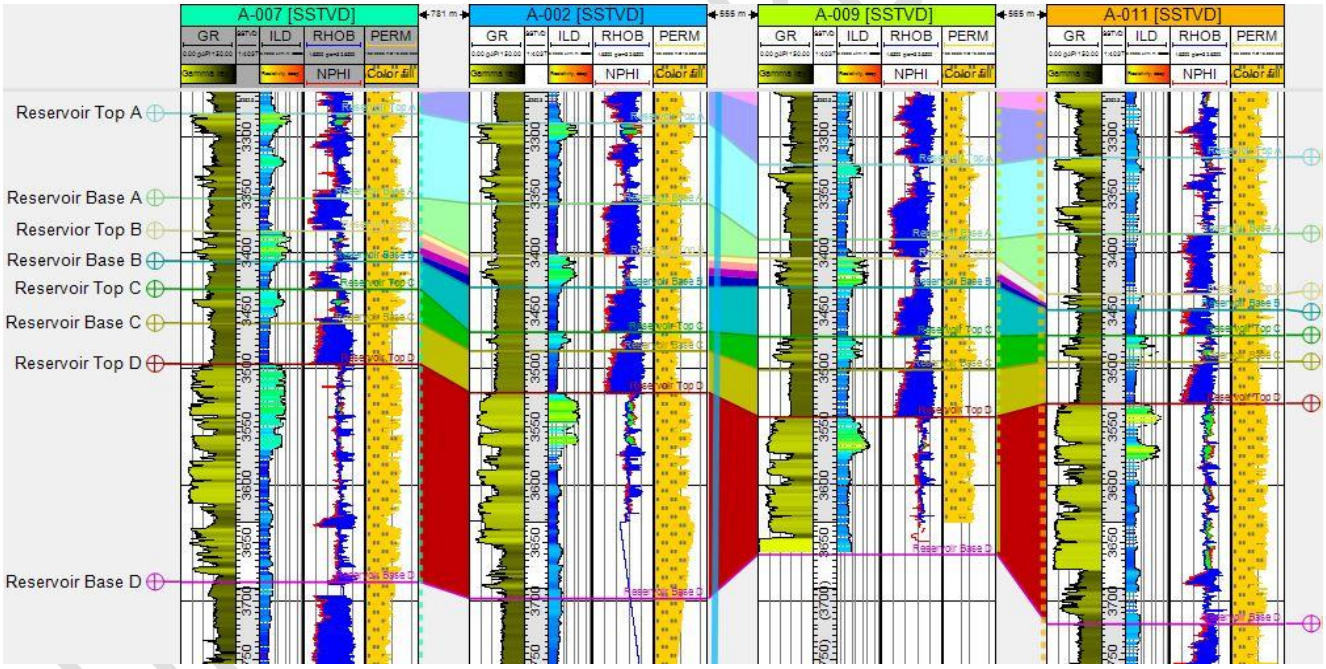

Figure 10: Permeability values calculated for the four reservoir intervals and correlated across all four wells.

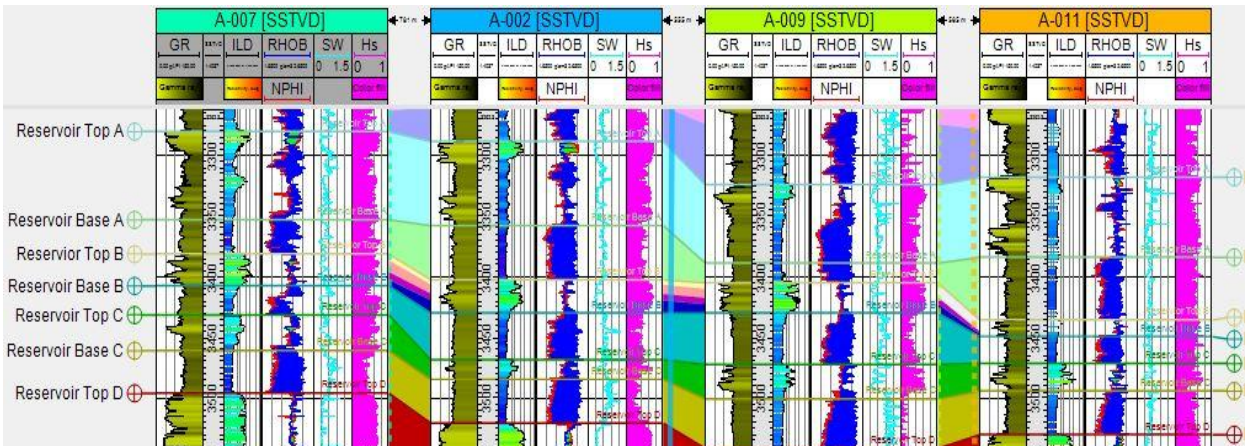

Figure 11: Hydrocarbon saturation calculated for the four reservoir intervals and correlated across all four wells.

Lithology and Fluid Discrimination

Cross plotting of some selected rock properties and rock attributes was carried out and the following results were obtained. Firstly, a cross plot of Vp/Vs ratio against Acoustic impedance distinguishes the A-011 reservoir into sand zone, shaly-sand zone, and shale zone. Secondly, lambda-rho (incompressibility) against Vp/Vs discriminates the reservoir of interest in sands and shale/sand/shale sequences. Next was the cross plot of Mu-rho against density, and finally, the cross plots of lambda-rho (λρ) against mu-rho (μρ) shows separation of four zones that can be inferred to be probable shale, brine, and gas zone confirmed by lowest density values.

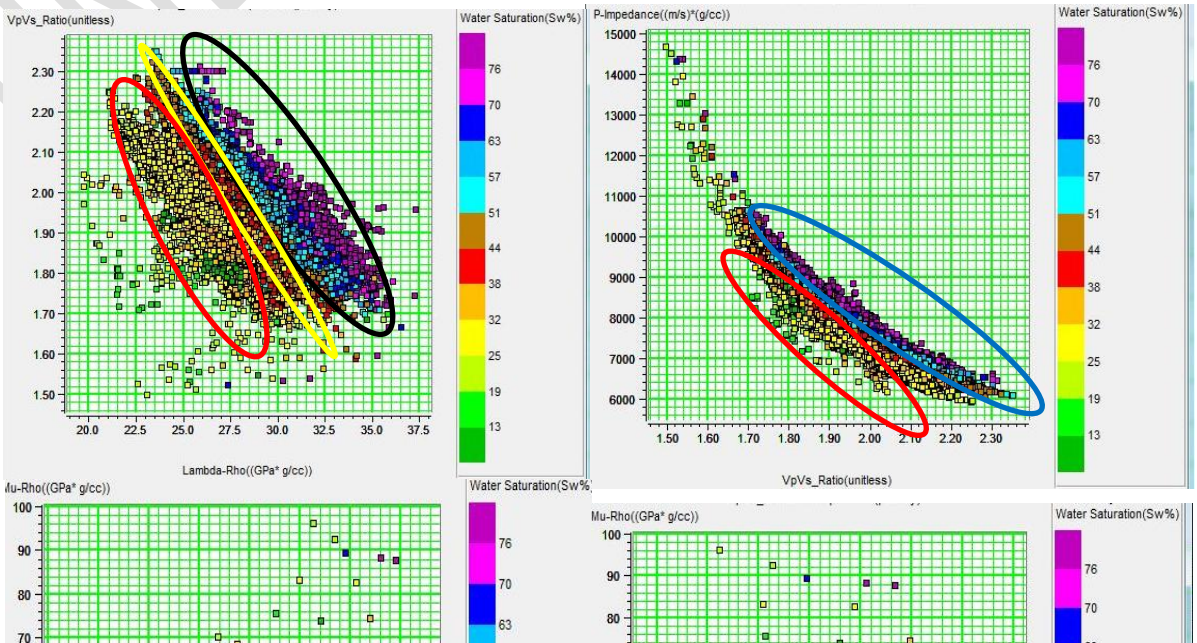

Figure 12: Cross plots for attributes computed to identify lithology and fluid discrimination using water saturation colour for Well 11.

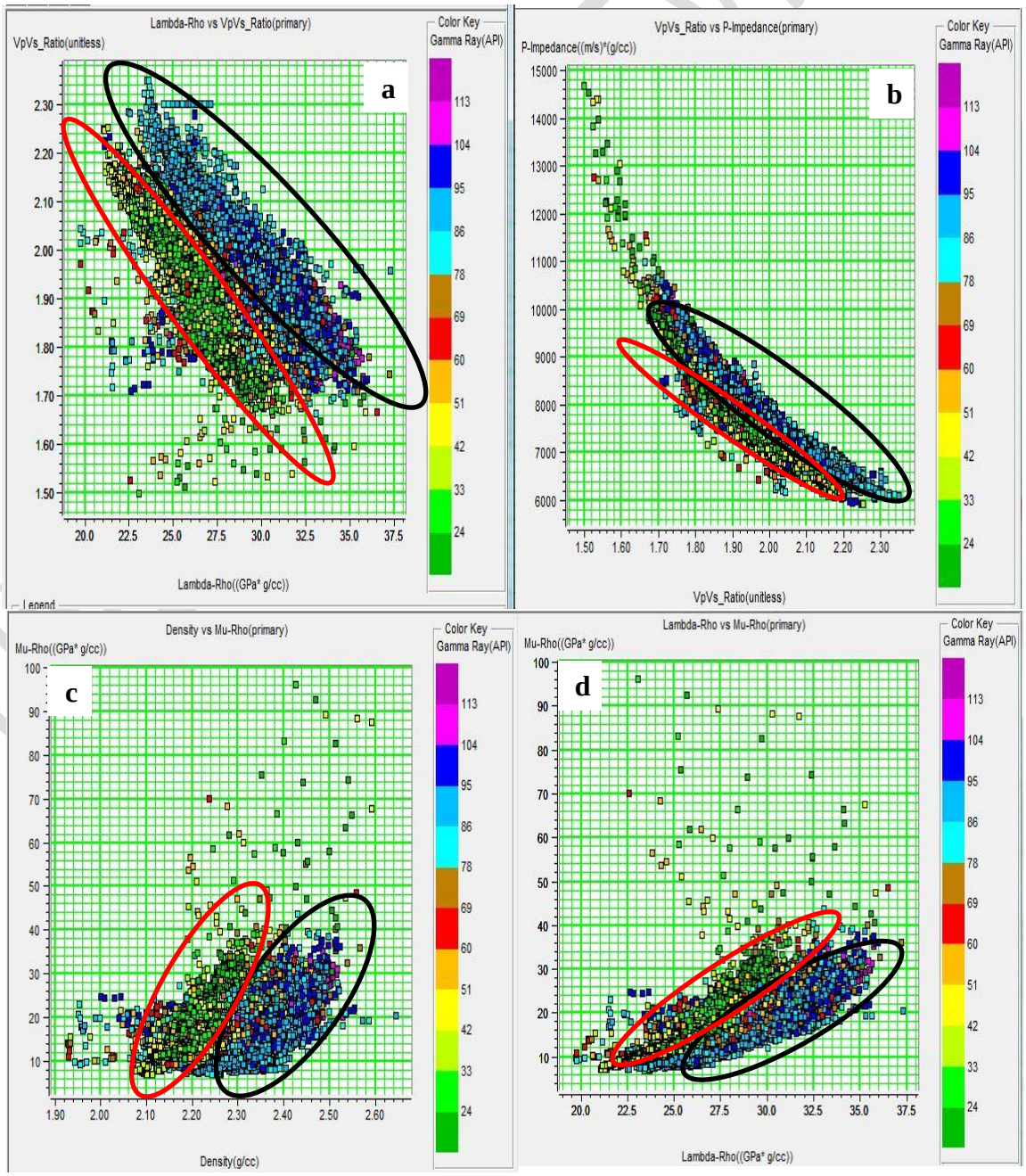

Figure 13: Cross plots for attributes computed to identify lithology discrimination using gamma ray colour key for Well 11.

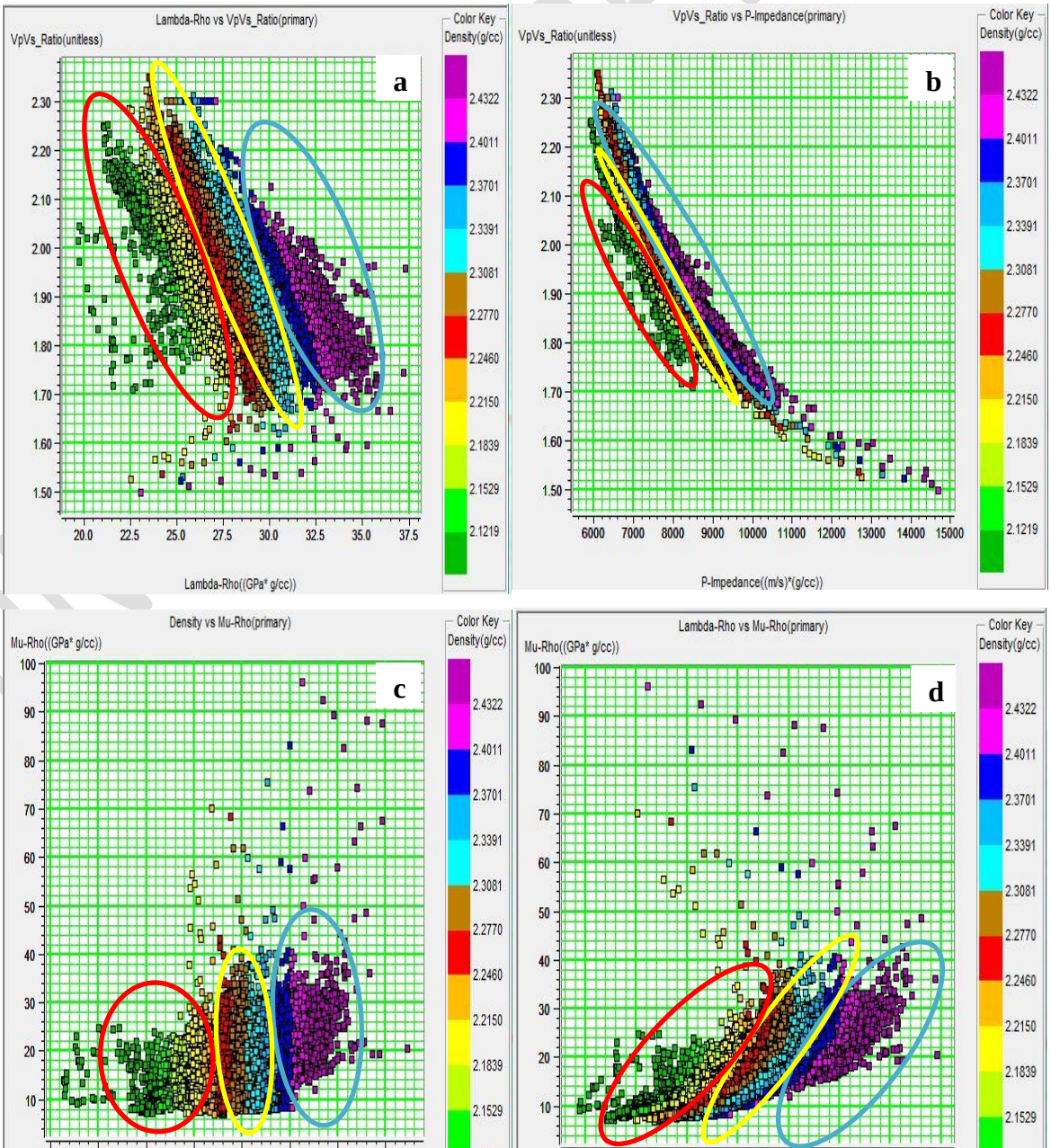

Figure 14: Cross plots for attributes computed to identify fluid and lithology discrimination using density colour key for Well 11.

Discussion

Petrophysical Reservoir Analysis

Figure 6a-d and 7 shows the mapped reservoirs in wells, with the associated petrophysical parameter logs while table 2 gives a summary of the reservoir details encountered in the well.

The four main reservoir units were identified (namely reservoirs A, B, C and D) across the wells (Figure 7, 8, 9, 10 and 11). The reservoir sand units range from about 16m to 177m thickness in Well A-002, 26m to 188m thickness in Well A-007, 26m to 118m thickness in Well A-009 and from 14m to 189m thickness in Well A-011 respectively. These reservoir units are generally made up of fairly clean sands, with an average shale volume that ranges from about 12.75% to 18.5%, average total and effective porosity ranging from 18.5% to 25.75% and 16.75% to 22.5% respectively, while the average water saturation ranges from about 54.25% to 68.75%. Reservoirs A and D shows signatures depicting block with sharp top and base sequence, reservoirs B show signatures depicting a fining downward with sharp base, while reservoir C show a coarsing upward with sharp top sequences on both ends of the shale beds. Reservoir B was observed to house the cleanest sand unit within the reservoirs.

Cross Plots Analysis

It was observed that both mu-rho and density are lithology discriminators, with density also being a fluid discriminator, the Mu-rho values are high for sand and low for shale. Conversely, the density of shale is higher than that of sand. Figure 12a, shows the variation of lambda-rho (incompressibility) against Vp/Vs for sands and shale/sand/shale sequences. The plots are better aligned towards the lambda rho axis, thus making lambda rho a better lithology discrimination tool. The black ellipse describes the shale zone, the yellow describes brine sand, and the red ellipse describes hydrocarbon sand. The cross plot of Vp/Vs ratio against Acoustic impedance (Zp) (Figure 12b), distinguishes the A-011 reservoirs into two zones namely; hydrocarbon sands (red ellipse), and shale zone (blue ellipse). This cross plot shows better fluid discriminator as well as lithology discrimination along the acoustic impedance axis, indicating that the acoustic impedance attribute will better describe the A-011 reservoir conditions in terms of lithology and fluid content than Vp/Vs ratio. In the cross plot of Mu-rho against density (Figure 12c), furthermore, brine is denser than hydrocarbon (oil and gas). Thus, the red ellipse in the figure 12c indicates hydrocarbon bearing sand, the yellow ellipse shows the brine saturated sand region, while the black section describes the shale region. Cross plots of lambda-rho ($\lambda\rho$) against mu-rho ($\mu\rho$) in Figure 12d, shows separation into four zones that can be inferred to be probable shale (black eclipse), brine (yellow eclipse), oil (red eclipse) and gas zone (blue eclipse) confirmed by lowest water saturation values. The plot indicates that $\lambda\rho$ is more robust than $\mu\rho$ in the analysis of fluids in the field of study and that $\mu\rho$ values are relatively low for the reservoir sand. The Acoustic impedance (Zp), Lambda-rho ($\lambda\rho$), Mu-rho ($\mu\rho$), and Poisson impedance (PI) attributes were found to be most robust in lithology and fluid discrimination within the reservoir in the

cross-plot analysis. The λ-μ-ρ technique was able to identify hydrocarbon sands, because of the separation in responses of both the λρ and μρ sections to hydrocarbon sands versus shale. Many different lithologies could also be identified by the cross plot of λρ versus μρ. This is possible because each lithology has a different rock properties response subject to fluid content and mineral properties. The cross plots for computed attributes to discriminate for lithology discrimination from Vp/Vs ratio against lambda-rho (λρ), acoustic impedance (Zp) against Vp/Vs ratio, Mu-rho (μρ) against density and mu-rho against lambda-rho (λρ) in Figure 13 for well 11 depicts that in the reservoirs the lithologies are majorly sands and shale predominantly found in Niger Delta. For Figure 14, the cross plots of Vp/Vs ratio against lambda-rho (λρ), Vp/Vs ratio against acoustic impedance (Zp), mu-rho (μρ) against density and mu-rho (μρ) against lambda-rho (λρ) depicts that in the reservoirs the fluid discriminates the blue eclipse as shale area, yellow eclipse as brine sands and red eclipse as oil.

Vp/Vs ratio against Lambda-rho

The cross plots of Vp/Vs ratio against Lambda-rho from petrophysical properties (gamma ray, water saturation and density) clearly show the distinct discrimination of probable hydrocarbon zones from the brine/shale zones within well A-011 (Figure 12a – 14a). From the cross plot, it was observed that the hydrocarbon zones correspond to low Lambda-Rho and high Vp/Vs ratio while brine/shale zones correspond to high Lambda-rho and low Vp/Vs ratio.

Vp/Vs ratio against P-impedance

The cross plots of P-impedance against Vp/Vs ratio from petrophysical properties (gamma ray, water saturation and density) clearly show the distinct discrimination of probable hydrocarbon sand zones from the shale zones within well A-011 (Figure 12b - 14b). From the cross plot, it

was observed that the hydrocarbon sand zones correspond to high P-impedance and low Vp/Vs ratio while shale zones correspond to low P-impedance and high Vp/Vs ratio.

Mu-rho against Density

The cross plots of Mu-rho against density from petrophysical properties (gamma ray, water saturation and density) clearly show the distinct discrimination of probable hydrocarbon sand zones from the shale zones within well A-011 (Figure 12c – 14c). From the cross plot, it was observed that the hydrocarbon sand zones correspond to high mu-rho and low density while shale zones correspond to low mu-rho and high density.

Mu-rho against Lambda-rho

The cross plots of Mu-rho against Lambda-rho from petrophysical properties (gamma ray, water saturation and density) clearly shows the distinct discrimination of probable hydrocarbon zones from the brine/shale zones within well A-011 (Figure 12d – 14d). From the cross plot, it was observed that the hydrocarbon zones correspond to high mu-rho and low lambda-rho while brine/shale zones correspond to low mu-rho and high lambda-rho.

CONCLUSION

The study used the results obtained from the well logs evaluation, well log correlation, petrophysical analysis and the cross plots analysis, to delineate the lithology and discriminate the reservoir fluids in other to characterized our study area, A-Field, onshore Niger Delta . In the reservoir delineation, four lithologic sand reservoirs were identified using gamma ray log, resistivity log and the cross plot of neutron and density logs. The study evaluated the following

petrophysical parameters for the field as follows, average effective porosity of 18.4%, total porosity estimated to be 20.25%, the average shale volume of 61.75%, average water saturation of 53.5% and permeability of 1508.0425mD respectively, these parameters were used to further quantify the extends of producibility of the four reservoirs.

Cross plots of computed extracted attributes were used to accurately delineate the lithology and discriminate the fluids, so as to further characterize the existence of fluid and lithology in the reservoir.

The quantitative interpretation of the reservoir characterization of A-field has revealed that the use of estimated petrophysical parameters of the rock properties as reservoir characterization technique was an effective technique, especially for fluid and lithology discrimination of the field in any given reservoir study. This study has also shown that A-field is not commercially viable in terms of hydrocarbon exploitation within the reservoir intervals studied because of the high-water saturation and shale volume values estimated, which are not highly economical for production of the field.

COMPETING INTERESTS DISCLAIMER:

Authors have declared that no competing interests exist. The products used for this research are commonly and predominantly use products in our area of research and country. There is absolutely no conflict of interest between the authors and producers of the products because we do not intend to use these products as an avenue for any litigation but for the advancement of knowledge. Also, the research was not funded by the producing company rather it was funded by personal efforts of the authors.

REFERENCES

Aamir, R., David, W. E., McDougall, A. and Pedersen P. K. (2016). Reservoir Characterization Using Microseismic Facies Analysis Integrated with surface seismic attribute, SEG The Leading Edge 4(2): 1 - 260.

Adel, A. A. (2013). Seismic Attributes Techniques to delinate channel complex in pliocene age, North Abu Qir, Nile Delta; . *Eygpt Journal of applied science Research 10 (2)*, 4255-4270.

Aizebeokhai, K. D. (2015). Seismic Attributes Analysis For Reservoir Characterization; Offshore Niger Delta. *Petroleum & Coal 57(6)*, 619-628.

Ajisafe, Y. A. (2013). 3-D Seismic Attributes for Reservoir Characterization of "Y" Field Niger Delta, Nigeria. *Journal of applied Geology and Geophysics (IOSR-JAGG)*, 23-31.

Bello, R., Igwenagu, C. L., & Onifade, Y. (2005). Cross plotting of Rock Properties for Fluid and Lithology Discrimination using Well. *Journal of Applied Science, Environnment and Manage*, 539-546.

Brown, A. R. (2011). Interpretation of Three-Dimensional Seismic Data, *Society of Exploration Geophysicists and American Association of Petroleum Geologists, 6th edition.*

Daukoru, C. M. (1994). Northern Delta Depobelt Portion of the Akata-Agbada Petroleum system, Niger Delta, Nigeria, Petroleum Association System, AAPG memoir 60. *American Association of Petroleum Geologists, Tulsa (AAPG)*, 598-616.

Doust, H. and Omotsola, E. (1990). Niger Delta, *in* Divergent passive Margin basins. *American Association of Petroleum Geologists,*, 239-248.

Ekweozor C. M., (1984). Petroleum Source-Bed Evaluation of Tertiary Niger Delta; *AAPG Bulletin, (68)*, 387-394.

Evamy, B.O., Herembourne, J., Kameline, P., Knap, W.A., Molloy, F.A. and Rowlands, P.H. (1978). Hydrocarbon habitat of Tertiary Niger Delta. *American Association of Petroleum Geologists Bulletin*, 62, 1-39

Iske A. and Randen T. (2005). Mathematical Methods and Modeling in Hydrocarbon exploration and Production. Schlumberger, Springer Publication

Lowrie, W. (2007). *Fundamentals of Geophysics*. London: Cambriodge University Press.

Goodway, B., Chen, T. and Downton, J. (1997). "Improved AVO fluid detection and lithology discrimination using Lame Petrophysical parameters; λ, μ and λ/μ fluid stack from P-wave and S-wave Inversion. Presented at 67th Annual International Meeting, Society of Exploration Geophysics (SEG) Expanded Abstract, 183-186, 1997

Olowokere, M. T. and Ojo, J. S. (2010). "Fluid Detections and Lithology Discrimination using Lame Petrophysical Parameters from Simultaneous Inversion – using Northern North Sea, Norway". National Association of Petroleum Explorationists (NAPE) Int'l Bulletin, 22(1), 36-42, 2010.

Omudu, L. M., Ebeniro, J. O. and Osayande, N. (2008). Cross-plot and Discriptive Statistic for Lithology and Fluid Discrimination – A case study from Onshore Niger Delta. National Association of Petroleum Explorationists (NAPE) International Bulletin, 20(2), 31-37.

Omudu, L. M., Ebeniro, J. O., Xynoglass, M. and Osayande, N. (2008). Fluid Discriminator Factor, Moduli Ratio and Reservior Characterization – A Niger Delta Experience". National Association of Petroleum Explorationists (NAPE) International Bulletin, 20(2), 38-44.

Opara, A.I., Anyiam, U.O., Nduka, A.V. (2011). 3D Seismic Interpretation and Structural Analysis of Ossu Oil Field, Northern Depobelt, Onshore Niger Delta, Nigeria. *The Pacific Journal of Science and Technology*. 12(1), 8pp.

Oyeyemi, D. K. and Aizebeokhai, P. A., (2015). Seismic Attribute Analysis for Reservoir Characterization; Offshore Niger Delta. *Petroleum and Coal 57(6)*, 619-628.

Perveiz, K. N. (2016). An Integrated Seismic Interpretation and Rock Physics attributes analysis for pore fluid discrimination. *Arabian Journal for Geoscience and Engineering, 41(1)*, 191-200.

Reijers, T. P. (1997). The Niger Delta Basin,. *Elsevier Science,* 151-172.

Russell, B. H., Hedlin, K., Hitterman, F. J. and Lines, L. R. (2003). Fluid property discrimination with AVO, A Biot- Grassmann perspective". Geophysics, 68, 29-39.

Sheriff, R.E., Telford, W.M., Geldart, L.P. (1980). Applied Geophysics 2nd Ed, Cambridge University Press

Short, K. and Stauble A. J. C, (1967) "Outline of Geology of the Niger delta," *The American Association of Petroleum Geologists Bulletin, 51,* 761–779.

Sofolabo, A. O., Ehirim, C. N. and Dagogo. T. (2018). Cross plot analysis of Extracted Seismic inversion attributes for fluid and Lithology discrimination: A case study of K-Field, Onshore Niger Delta Area, Nigeria". International Journal of Science and Research (IJSR). 7(4), 804-810, 2018.

Stacher, P. (1995). Present understanding of the Niger delta hydrocarbon habitat: Geology of Deltas. *AA Balkema, Rotterdam,* 257–267

Subrata, B., Sunil, S., Prabir, N., Afrah, A., Sarah, A., and Abdulaziz, A. (2017). Identification of Thin Carbonate Reservoir Facies through Integrated Seismic Attribute Analysis: A Case Study of Kuwait, *The Leading Edge SEG, 6093.*

Tuttle, M. L. W., Charpentier R. R. and Brownfield M. E. (1999). "The Niger delta petroleum system: Niger delta province, Nigeria, Cameroon, and Equatorial Guinea, Africa, 99-50.

Van Bemmel, P.P. and R.E.F. Pepper (2000). Seismic signal processing method and apparatus for generating a cube of variance values. U.S Patent 6,151,555.

Weber, K. J. (1975). Petroleum Geology of the Niger Delta:. *Proceedings of the Ninth World Petroleum Congress, 2, Geology:* London: Applied Science Publishers, Ltd., 210-221

Weber, K. J. and Daukoru, E. M. (1975). Petroleum Geology of the Niger Delta; *Earth Science Journal, 2 (1),* 210-221.